



Mathematical Modeling of Blood Flow Through a Stenosed Bifurcated Artery With Heat Source and Magnetic Effect

G. Madhava Rao^{*1} , D. Srinivasacharya²  and G. Venkata Suman³ 

¹Department of Mathematics, Malla Reddy University, Hyderabad 500100, Telangana, India

²Department of Mathematics, National Institute of Technology, Warangal 506004, Telangana, India

³Department of Mathematics, Malla Reddy University, Hyderabad 500100, Telangana, India

Received: May 27, 2021

Accepted: August 2, 2021

Abstract. The present article illustrates the influence of heat source on MHD blood flow in a branched artery with small obstacle in its main artery by treating blood as micropolar fluid. Artery forming branch is presumed as straight cylinder of restricted length and is symmetric about its axis. The irregular shape of constricted branched artery is changed to a well defined shape by utilizing a radial coordinate transformations. Numerical solution is computed for interested physical quantities such as rate of flow, and shearing stress on one as well as the other sides of the apex.

Keywords. Blood flow, Micropolar fluid, Branched artery, Mild constriction, MHD, Heat source

Mathematics Subject Classification (2020). 76A05; 74S20

Copyright © 2021 G. Madhava Rao, D. Srinivasacharya and G. Venkata Suman. *This is an open access article distributed under the Creative Commons Attribution License, which permits unrestricted use, distribution, and reproduction in any medium, provided the original work is properly cited.*

1. Introduction

The investigation of fluid dynamics properties of biological systems such as human arterial system with respect to the development of mild constriction in the artery has been main object of research fraternity in recent years. Construction occurring due to fatty material development inside the artery. The happening of constriction depends on shape of the artery, in general at branches, curvatures given in Chatzizisis [1]. Once constriction is happened, the bio-mechanical properties associated with blood flow are naturally changed.

***Email:** rao.gmr.madhav@gmail.com

Micropolar fluid model consists of substructure and micromotion of the fluid elements, is introduced by Eringen [3]. Shit and Roy [7] explored the pulsatile behavior of flow of blood over a constricted artery in existence of magnetic field. Bourhan and Ahmad [10] illustrated the impact of magnetic field on blood flow characteristics in a multi-stenosed artery. Prakash *et al.* [6] investigated variations in temperature with Prandtl number, heat source parameter. An impact of heat transfer on flow of blood in artery with porous wall has been presented by Ogulu and Abbey [5]. Ellahi *et al.* [2] studied the characteristics of micropolar fluid over a constricted artery with heat and mass transfer. Srinivasacharya and Rao [8] examined influence of bifurcation angle on flow rate and shear stress. Impact of magnetic field and pulsatile pressure gradient on flow of micropolar fluid has been studied by Srinivasacharya and Rao [9]. Sabaruddin and Ismail [4] investigated the velocity profile, temperature profile and streamline pattern at various locations considering effect of Reynold numbers to the blood flow.

2. Mathematical Formulation

Micropolar fluid model for blood in branched artery with constriction in the main part is considered under magnetic effect and heat source with coordinate system (r, z, t) as shown in Figure 1. Flow is considered as symmetric, this implies all variables are self-sufficient with respect to θ . Therefore, equations governing the flow are

$$-\frac{\partial p}{\partial z} + \frac{\kappa}{r} \frac{\partial}{\partial r}(rv) + (\mu + \kappa) \frac{1}{2} \frac{\partial}{\partial r} + \rho g \beta_2 (T - T_i) - \sigma B_0^2 w = 0, \quad (2.1)$$

$$-2k\nu - \kappa \frac{\partial w}{\partial r} + \gamma \frac{\partial}{\partial r} \left(\frac{1}{r} \frac{\partial}{\partial r}(rv) \right) = 0, \quad (2.2)$$

$$\frac{k_0}{\rho c_p} \left(\frac{1}{r} \frac{\partial}{\partial r} \left(r \frac{\partial T}{\partial r} \right) \right) + \frac{Q_1}{\rho c_p} (T - T_i) = 0, \quad (2.3)$$

where w is axial velocity components, v is component of microrotation vector, ρ and j are the fluid pressure, thickness and microgyration parameter, respectively. T_i speaks for the temperature on internal wall, c_p speaks for the specific heat, Q_1 speaks for heat breeding, B_0 is the strength of magnetic field applied.

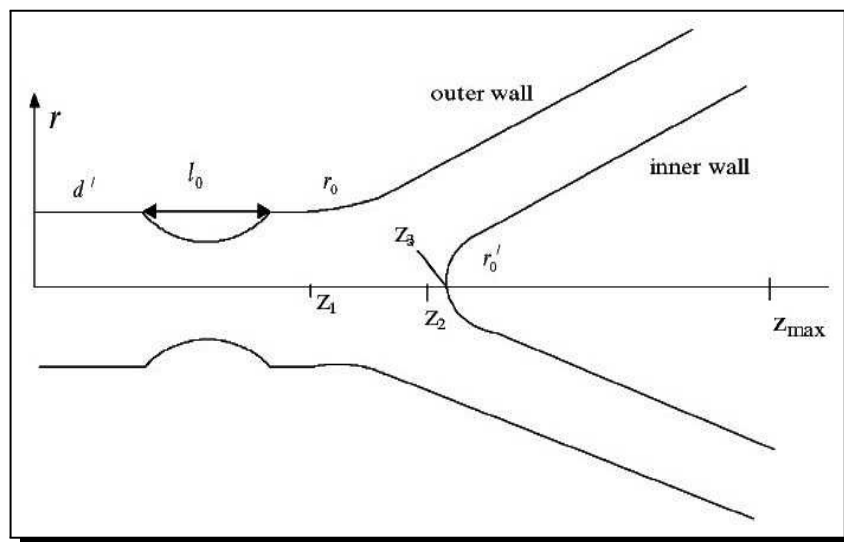


Figure 1. Geometry of a branched artery with mild constriction

The mathematical representation for the walls outside and inside to the artery with slight constriction in its parent artery are given by

$$R_1(z) = \begin{cases} c, & 0 \leq z \leq b' \text{ and } b' + b_0 \leq z \leq z_1 \\ \left(c - \frac{4}{l_0^2} (l_0(z - b') - (z - b')^2) \right), & b' \leq z \leq b' + b_0 \\ (c + r_0 - \sqrt{r_0^2 - (z - z_1)^2}), & z_1 \leq z \leq z_2 \\ (2r_1 \sec \beta + (z - z_2) \tan \beta), & z_2 \leq z \leq z_{\max} \end{cases} \tag{2.4}$$

$$R_2(z) = \begin{cases} 0, & 0 \leq z \leq z_3 \\ \sqrt{(r'_0)^2 - (z - z_3 - r'_0)^2}, & z_3 \leq z \leq z_3 + r'_0(1 - \sin \beta) \\ (r'_0 \cos \beta + z_4), & z_3 + r'_0(1 - \sin \beta) \leq z \leq z_{\max} \end{cases} \tag{2.5}$$

where c and r_1 are radii of the main artery at non-constricted position and child artery, r_0, r'_0 represents radii of curvatures at start of lateral junction and division of branched artery, b is length of mild constriction in parent artery, z_1 and z_2 represent locations of start of onset and offset of lateral junction, z_3 represent apex, τ_m is peak of the constriction at $z = b' + b_0/2$, β is 50% of bifurcation angle and z_{\max} is the finite dimension of the artery. To make, all variables as dimensionless, following data have been used

$$\left. \begin{aligned} r = c\bar{r}, w = w_0\bar{w}, p = \frac{Lw_0\mu\bar{p}}{c^2}, z = L\bar{z}, v = \frac{w_0\bar{v}}{c}, j = c^2\bar{j}, b = L\bar{b}, \Theta = \frac{T - T_i}{T_o - T_i}, \\ R_1(z) = c\bar{R}_1(\bar{z}), R_2(z) = c\bar{R}_2(\bar{z}), r_1 = c\bar{r}_1, z_1 = c\bar{z}_1 \end{aligned} \right\} \tag{2.6}$$

where L is unique length, T_0 is temperature on the external wall of the branched artery and w_0 is characteristic velocity.

Use eq. (2.8) into eq. (2.2) to eq. (2.4) and dropping tildes, we have

$$-\frac{\partial p}{\partial z} + \left(\frac{N}{1-N} \right) \frac{1}{r} \frac{\partial}{\partial r} (rv) + \left(\frac{1}{1-N} \right) \frac{1}{r} \frac{\partial}{\partial r} \left(r \frac{\partial w}{\partial r} \right) + \frac{G_r}{Re} \theta - H^2 w = 0, \tag{2.7}$$

$$-2v - \frac{\partial w}{\partial r} + \left(\frac{2-N}{m^2} \right) \frac{\partial}{\partial r} \left(\frac{1}{r} \frac{\partial}{\partial r} (rv) \right) = 0, \tag{2.8}$$

$$\frac{1}{r} \left(\frac{\partial}{\partial r} \left(r \frac{\partial \Theta}{\partial r} \right) \right) + s\Theta = 0, \tag{2.9}$$

where $G_r = \frac{\rho^2 g \beta_1 c^3 (T_o - T_i)}{\mu^2}$ represents the Grashof numeral, $Re = \frac{\rho c w_0}{\mu}$ represents Reynolds numeral, $H = B_0 c \sqrt{\frac{\sigma}{\mu}}$ represents the Hartmann numeral, $s = \frac{Q_1 c^2}{k_0}$ is Heat source character, $N = \frac{\kappa}{\mu + \kappa}$ represents micropolar coupling numeral ($0 \leq N \leq 1$) and $m^2 = \frac{c^2 \kappa (2\mu + \kappa)}{\gamma(\mu + \kappa)}$ is micropolar character.

The corresponding boundary conditions in dimensionless form are

$$\left. \begin{aligned} \frac{\partial w}{\partial r} = 0, \Theta = 0, v = 0 & \text{ on } r = 0 \text{ for } 0 \leq z \leq z_3 \\ w = 0, \Theta = 1, v = 0 & \text{ on } r = R_1(z) \text{ for all } z \\ w = 0, \Theta = 0, v = 0 & \text{ on } r = R_2(z) \text{ for } z_3 \leq z \leq z_{\max} \end{aligned} \right\} \tag{2.10}$$

The influence of $R_1(z)$ and $R_2(z)$ is assigned into equations (2.7), (2.8), (2.9) and (2.10) by using the coordination mapping [7]

$$\xi = \frac{r - R_2}{R}, \quad \text{where } R = R_1 - R_2 \quad (2.11)$$

With this mapping, equations (2.7), (2.8), (2.9) and (2.10) take the form

$$-\frac{\partial p}{\partial z} + \frac{N}{1-N} \left(\frac{1}{R} \frac{\partial v}{\partial \xi} + \frac{v}{\xi R + R_2} \right) \frac{1}{1(1-N)R^2} \left[\frac{\partial^2 w}{\partial \xi^2} + \frac{R}{\xi R + R_2} \frac{\partial w}{\partial \xi} \right] + \frac{G_r}{R_e} \Theta - H^2 w = 0, \quad (2.12)$$

$$-\frac{1}{R} \frac{\partial w}{\partial \xi} + \frac{(2-N)}{m^2 R^2} \left[\frac{\partial^2 v}{\partial \xi^2} + \frac{R}{(\xi R + R_2)^2} v + \frac{R}{\xi R + R_2} \frac{\partial w}{\partial \xi} \right] - 2v = 0, \quad (2.13)$$

$$\frac{1}{R^2} \frac{\partial^2 \Theta}{\partial \xi^2} + \frac{1}{R(\xi R + R_2)} \frac{\partial \Theta}{\partial \xi} + s\Theta = 0. \quad (2.14)$$

The transformed boundary conditions are

$$\left. \begin{aligned} \frac{\partial w}{\partial \xi} = 0, \quad \Theta = 0, \quad v = 0 & \quad \text{on } \xi = 0 \text{ for } 0 \leq z \leq z_3 \\ w = 0, \quad \Theta = 1, \quad v = 0 & \quad \text{on } \xi = 1 \text{ for all } z \\ w = 0, \quad \Theta = 0, \quad v = 0 & \quad \text{on } \xi = 0 \text{ for } z_3 \leq z \leq z_{\max} \end{aligned} \right\} \quad (2.15)$$

3. Method of Solution

The reduced equations (2.12)-(2.14) subject to the boundary conditions (2.15) are transformed into a tridiagonal system of equations by central difference scheme where each element is again a matrix. This system is dealt with block elimination method.

The physical measures to be interpreted are temperature, volume of flow and shear stress for the branched artery.

Flow rate in daughter artery Q_d and in parent artery Q_p are calculated by using

$$Q_p = 2\pi R \left[R \int_0^1 \xi w \, d\xi + R_2 \int_0^1 w \, d\xi \right]$$

and

$$Q_d = \pi R \left[R \int_0^1 \xi w \, d\xi + R_2 \int_0^1 w \, d\xi \right].$$

The wall shear stress along both the walls of the artery is given by

$$\tau = \frac{1}{1-N} \frac{dw}{dr} + \frac{N}{1-N} v.$$

4. Discussion

From Figure 2(a), it is observed that volume of flow is decreasing with a rise in s . Applications of heat source show the variations in volume of flow, this is useful for the thermal healing in the medication of tumor cysts, glands, etc. From Figure 2(b), it is evident that the volumetric volume of flow is decreasing with a rise in H . Hence, imposing magnetic field on flow of blood be used to control the volume blood flow during surgeries. Flow rate is fluctuation at apex rapidly because of back flow.

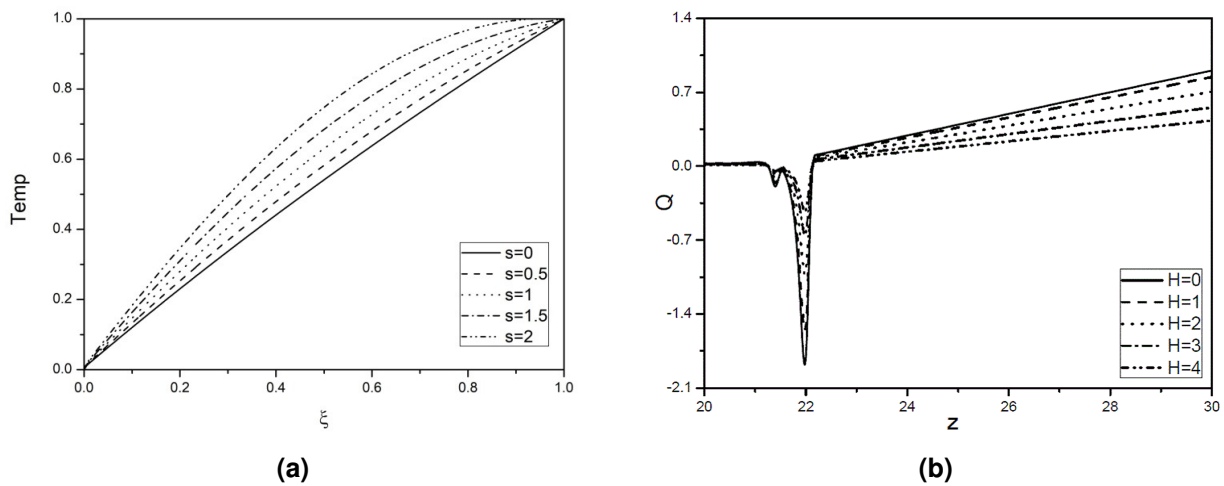


Figure 2. Impact of (a) s , and (b) H on volume of flow for fixed values of other parameters

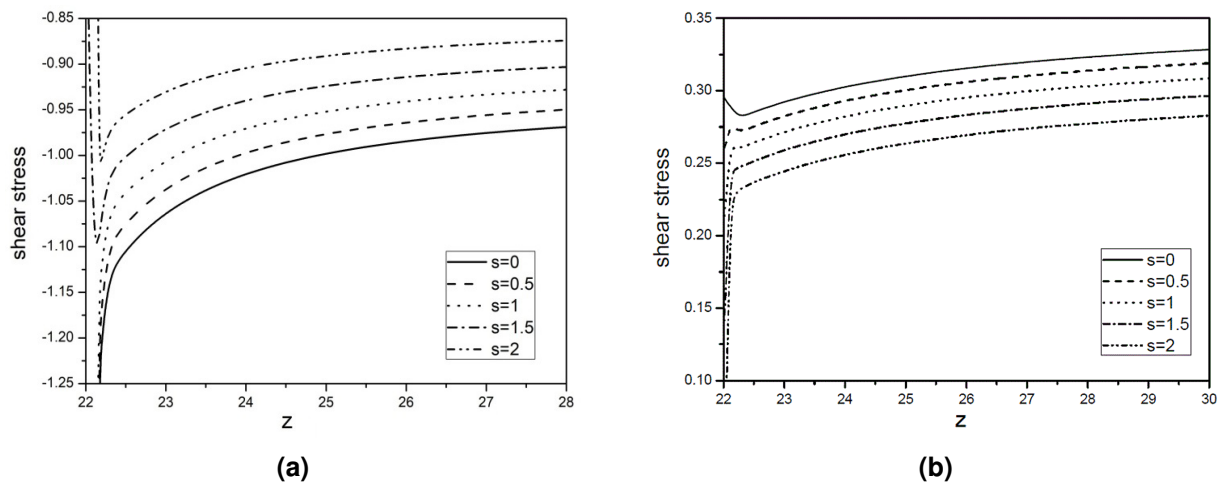


Figure 3. Impact of s on shearing stress in the onward direction of (a) internal and (b) outside walls of the daughter artery

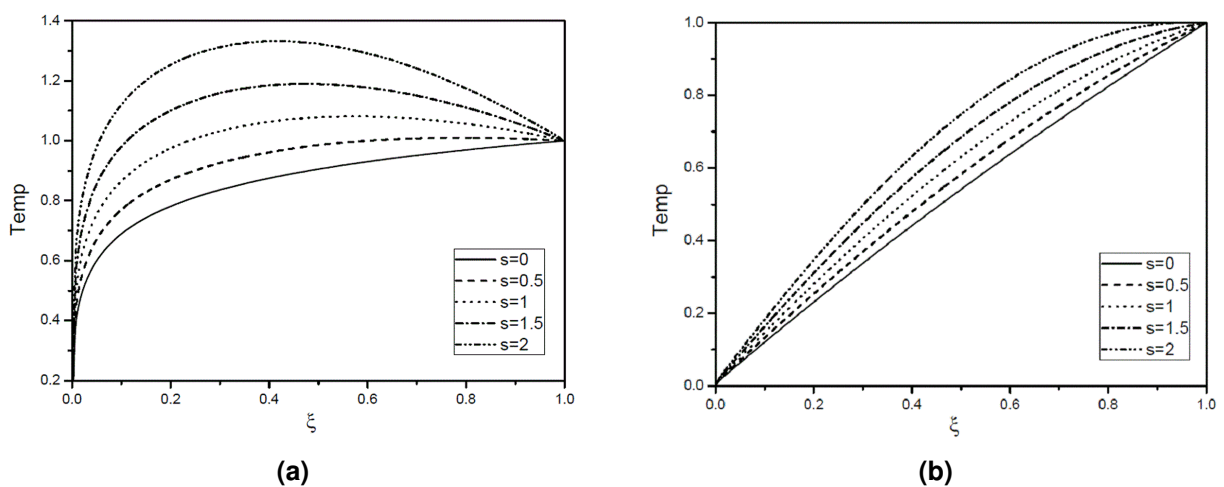


Figure 4. Influence of s on temperature (in degree Fahrenheit) both in (a) main and (b) child arteries with fixed values of other parameters

From Figure 3(a) and Figure 3(b) respectively explored, shearing stress τ is increasing in the onward direction of the internal wall while falling down in the onward direction of external wall of the child artery with a rise in s .

Figure 4(a) and Figure 4(b) show that the rise in s definitely increases the temperature rapidly in main and child arteries. But the impact is quite high in the parent artery.

5. Conclusions

The current work helps us to understand physically, the impact of s and H on volume of flow and shear stress of streaming blood over branched artery, this is very importance for medical science. Heat source is useful for the thermal healing in medication of tumor cysts, glands, etc. Imposing of magnetic field on flow of blood can be used to control volume of blood flow during surgeries.

Competing Interests

The authors declare that they have no competing interests.

Authors' Contributions

All the authors contributed significantly in writing this article. The authors read and approved the final manuscript.

References

- [1] Y. S. Chatzizisis and G. D. Giannoglou, Pulsatile flow: A critical modulator of the natural history of atherosclerosis, *Medical Hypotheses* **67**(2) (2006), 338 – 340, DOI: 10.1016/j.mehy.2006.02.005.
- [2] R. Ellahi, S. U. Rahman, S. Nadeem and Akbar, Influence of heat and mass transfer on micropolar fluid of blood flow through a tapered stenosed arteries with permeable walls, *Journal of Computational and Theoretical Nanoscience* **11** (2014), 1156 – 1163, DOI: 10.1166/jctn.2014.3475.
- [3] E. C. Eringen, Theory of micropolar fluids, *Journal of Mathematics and Mechanics* **16** (1966), 1 – 16, DOI: 10.1512/iumj.1967.16.16001.
- [4] M. S. A. Jamali and Z. Ismail, Simulation of Heat Transfer on blood flow through a stenosed bifurcated artery, *Journal of Advanced Research in Fluid Mechanics and Thermal Sciences* **60**(2) (2019), 310 – 323, URL: https://www.akademiabaru.com/doc/ARFMTSV60_N2_P310_323.pdf.
- [5] A. Ogulu and T. M. Abbey, Simulation of heat transfer on an oscillatory blood flow in an indented porous artery, *International Communications in Heat and Mass Transfer* **32** (2005), 983 – 989, DOI: 10.1016/j.icheatmasstransfer.2004.08.028.
- [6] O. Prakash, S. P. Singh, K. Devendra and Y. K. Dwivedi, A study of effects of heat source on MHD blood flow through bifurcated arteries, *AIP Advances* **1** (2011), 042128, 7 pages, DOI: 10.1063/1.3658616.
- [7] G. C. Shit and M. Roy, Pulsatile flow and heat transfer of a magneto-micropolar fluid through a stenosed artery under the influence of body acceleration, *Journal of Mechanics in Medicine and Biology* **11** (2011), 643 – 661, DOI: 10.1142/S0219519411003909.

- [8] D. Srinivasacharya and G. M. Rao, Magnetic effects on pulsatile flow of micropolar fluid through a bifurcated artery. *World Journal of Modelling Simulation* **12**(2) (2016), 147 – 160, URL: <http://www.worldacademicunion.com/journal/1746-7233WJMS/wjmsvol12no02paper06.pdf>.
- [9] D. Srinivasacharya and G. M. Rao, Micropolar fluid flow through a stenosed bifurcated artery, *Nonlinear Analysis: Modelling and Control* **22**(2) (2017), 147 – 159, DOI: 10.15388/NA.2017.2.1.
- [10] B. Tashtoush and A. Magableh, Magnetic field effect on heat transfer and fluid flow characteristics of blood flow in multi-stenosis arteries, *Journal of Heat Mass Transfer* **44** (2008), pp. 297 – 304, DOI: 10.1007/s00231-007-0251-x.

